

# The Automatic Phasing System for the Stanford Two-Mile Linear Electron Accelerator

C. B. WILLIAMS, A. R. WILMUNDER, J. DOBSON, H. A. HOGG, M. J. LEE, AND  
G. A. LOEW, MEMBER, IEEE

**Abstract**—This paper describes the system for automatically phasing 240 high-power klystrons that drive the Stanford two-mile linear electron accelerator.

After a brief discussion of the requirements of a phasing system for such a long machine and a review of some alternative methods which were initially considered, the principle of "Beam-Induction" phasing is described.

Advantages of the "Beam-Induction" technique are listed, and the problem of obtaining phase error information from accelerator signals varying over a 54-dB power range is considered. It is shown that the problem may be solved by the use of coaxial thermionic diodes, which have nearly linear detection characteristics.

The concept of phase-wobbling is introduced. It is shown that this idea may be used to design an ac servo system, avoiding problems with dc amplifier stability. Phase wobbling is also seen to remove phasing errors due to imperfect matching of the diode pair.

The installation and operation of the automatic phasing system in a typical sector of the machine is briefly described.

In conclusion, some results of preliminary tests on the first two sectors (660 feet) of the machine are presented.

## INTRODUCTION

THE AUTOMATIC phasing system for the Stanford two-mile linear electron accelerator is designed to be capable of adjusting the phases of 240 high-power klystrons so that they each contribute maximum energy to the bunched electron beam being accelerated. The accelerator is, at present, being built by Stanford University under contract with the U. S. Atomic Energy Commission. A two-mile long Klystron Gallery contains the 240 high-power klystrons and modulators and all the RF drive and local control equipment together with the electrical, vacuum, and water systems. The 10 000 foot accelerator structure is housed in a reinforced concrete building lying 25 feet below the Klystron Gallery. (See Fig. 1.) It consists of a cylindrical disk-loaded waveguide whose dimensions have been chosen so that it propagates a  $TM_{01}$  wave with a phase velocity equal to the velocity of light at 2856 Mc/s (10.5 cm wavelength). There are 960 sections, each 10 feet long, individually supplied with RF

power by means of a rectangular waveguide. They are grouped into 30 sectors, each containing 32 sections and a special 10 foot "drift section" in which the functions of beam steering, focusing, current monitoring, and position monitoring are performed. The accelerator is preceded by an injector, which contains an electron gun and special "buncher" sections for initial capture, bunching, and acceleration of the electron beam. At the end of the machine there is an elaborate "switchyard" through which the beam may be channeled to various experimental end-stations. Initial operation will be with the machine equipped according to the "Stage 1" design i.e., with one 24 MW klystron driving four 10-foot sections, making a total complement of 240 klystrons. Electron beam currents will be up to 300 mA peak, and electron energies will be as high as 20 GeV.

After a few feet of acceleration, the electron beam has for all practical purposes attained the velocity of light and is, therefore, in synchronism with the traveling wave in the disk-loaded waveguide. For maximum energy transfer, the phase of each klystron must be adjusted so that the electron bunches, upon entering the corresponding accelerator sections, ride the crest of the axial electric field wave  $E_z$ . [See Figs. 2 and 3(a)]. In a perfectly phased accelerator, each electron bunch will maintain this position relative to the RF wave in every section, arriving at the end of the machine with a maximum possible energy

$$V_{\max} = \sum_{n=1}^N V_n \quad (1)$$

where  $N$  is the number of accelerator sections and  $V_n$  is the maximum energy available from section  $n$  [Fig. 3(b).]

If the field is incorrectly phased so that when the electron bunch enters section  $n$  it is displaced from the crest  $E_{z\max}$  by a phase angle  $\phi_n$ , the accelerating force acting upon the electron bunch will be decreased by a factor  $\cos \phi_n$ . In general, the total energy gained in the accelerator will be

$$V_{\text{Tot}} = \sum_{n=1}^N V_n \cos \phi_n. \quad (2)$$

For small values of  $\phi_n$ , we may approximate this to

$$V_{\text{Tot}} = \sum_{n=1}^N V_n \left(1 - \frac{\phi_n^2}{2}\right). \quad (3)$$

Manuscript received May 6, 1965; revised August 23, 1965. The work reported in this paper was supported by the U. S. Atomic Energy Commission.

C. B. Williams is with the Laboratoire de l'accélérateur linéaire, Orsay, France. He is on leave from the Stanford University Linear Accelerator Center.

Messrs. Wilmunder, Hogg, Lee, and Loew are with the Stanford Linear Accelerator Center, Stanford University, Stanford, Calif.

J. Dobson is with the Department of Electrical Engineering, University of Sheffield, Sheffield, England. He was formerly with the Stanford University Linear Acceleration Center.

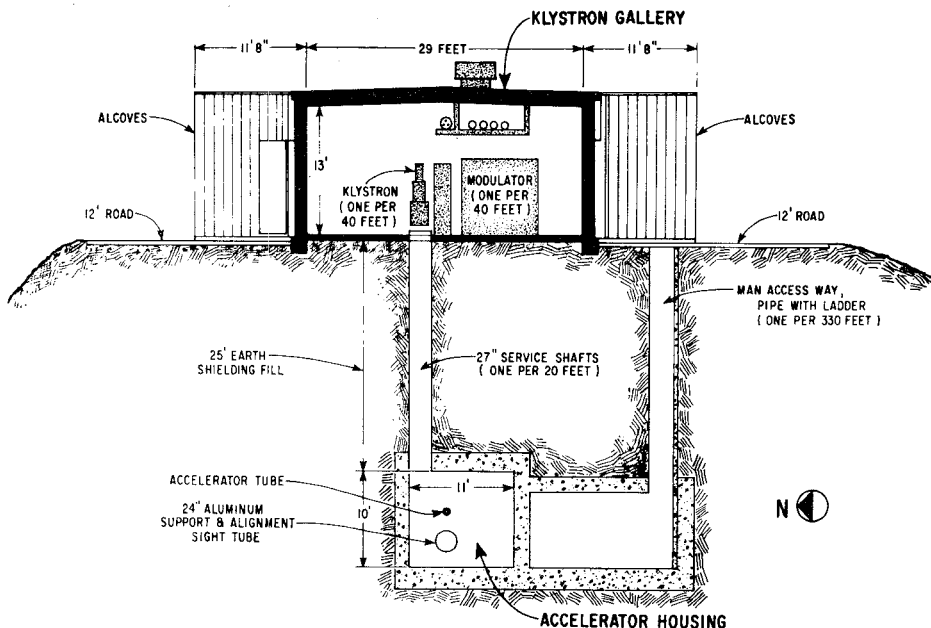


Fig. 1. Accelerator cross section; looking east in direction of beam.

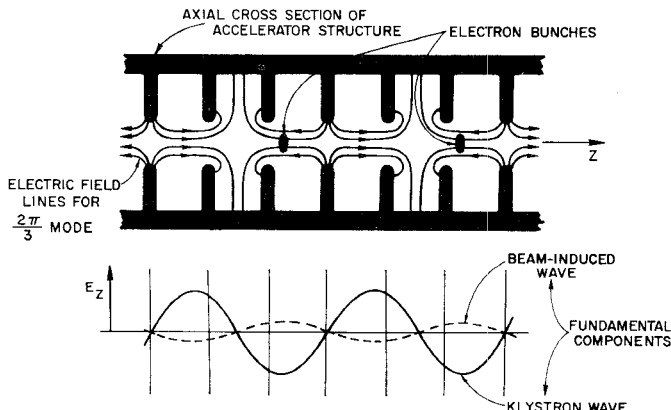


Fig. 2. RF field and electron bunch distribution in accelerator structure.

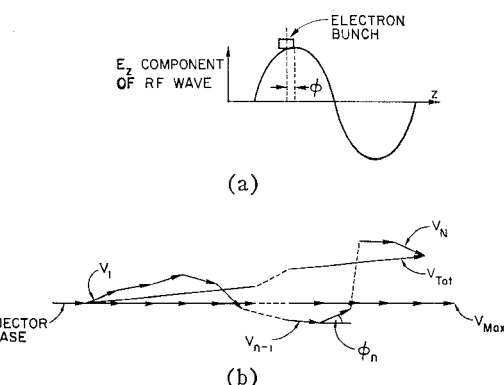
Assuming that the RF power into each section is the same, this becomes

$$V_{\text{Tot}} \simeq VN \left( 1 - \frac{\bar{\phi}^2}{2} \right) \quad (4)$$

where  $\bar{\phi}^2$  is the average value of  $\phi_n^2$ .

From (4) it is apparent that if we require the electron energy to be not less than 99.5 percent of the maximum value, then  $\bar{\phi}^2/2$  must be less than 0.005, or the rms phasing error must be less than 5 degrees. This phasing tolerance was initially adopted for the two-mile machine.

In addition to the stringent requirement that it shall be capable of adjusting the phase of the RF wave within  $\pm 5$  degrees of the electron beam phase at any point on the accelerator, the ideal phasing system must function rapidly and reliably, with the minimum interference with accelerator operation.

Fig. 3. Illustrating the effect of imperfect phasing.  $\phi$  is the phase angle of the central electron with respect to the wavecrest.

#### Early Methods Proposed and Their Limitations

Several methods for phasing the accelerator were considered in detail before the final choice was made. Two of these will be reviewed very briefly before proceeding to a detailed discussion of the adopted method.

The first method suggests itself immediately upon examination of Fig. 3(b): it involves simply rotating the phase of the RF wave in each section to maximize  $V_{\text{Tot}}$ . Unfortunately, this method's lack of sensitivity for a long accelerator with large  $N$  is also apparent. If we are to detect a change in phase of  $\pm 5$  degrees about the optimum for one klystron in 240, we must be prepared to measure an energy change of one part in 2750. From this it is clear that beam energy maximization is not a very good way of phasing a long machine. The sensitivity can be improved, however, by observing the current in part of the electron beam after dispersion by a spectrometer magnet [1].

Phasing may also be done by measuring the change in

reactive beam loading as the relative phases of beam and RF wave are changed in an accelerator section. For a detailed discussion, see [2]–[7].

This method is based on the fact that when the electrons are in the correct position on the RF wave, i.e., “riding the crest” as shown in Fig. 2(a), the phase of the output from the accelerator section is the same with the beam on or off. This can be seen from Figs. 2(b) and 4.

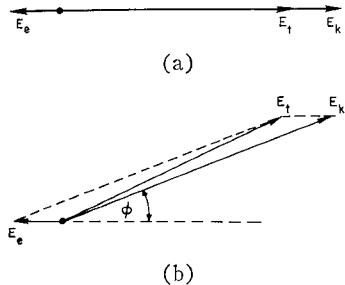


Fig. 4. Vector diagram illustrating principle of phasing accelerator section by reactive beam loading method. (a) Orientation of field vectors when phasing is correct. (b) Orientation of field vectors when phasing is incorrect.

When the electron bunches are correctly phased with respect to the high-power accelerating RF wave, the RF wave *induced* in the accelerator by the electron bunches is such that the fundamental space harmonic of the accelerating and induced waves is 180 degrees out of phase [Fig. 2(b)]. Thus the resultant wave  $E_t$  [Fig. 4(a)] is in phase with the accelerating (klystron) wave,  $E_k$ . When the bunch “slips” with respect to the klystron wave, a phase shift develops between the klystron and resultant waves, as shown by the vector diagram [Fig. 4(b)]. Thus, by installing a phase bridge between the input and output of the accelerator section, the phase difference between the output wave with the beam off and the output wave with the beam on may be measured and reduced to zero, either manually or automatically.

This method of accelerator phasing is quite feasible, but the sensitivity depends on the beam current and the klystron power, and it does require that the beam be turned on and off, thus interfering with physics experiments.

#### SELECTED METHOD OF PHASING

##### *Phasing by the “Beam-Induction Technique”*

Examination of the latter method of phasing, which involves an indirect measurement of the phase of the beam-induced wave in an accelerator section, leads us to the *beam-induction* method which has been chosen for the two-mile machine.

The principle of the beam-induction technique is as follows:

- 1) With the klystron wave turned off, the phase of the beam-induced wave in the particular accelerator section to be phased is compared with a coherent reference signal of the same frequency.

- 2) The phase of the *reference* signal is adjusted to the same phase as the beam-induced signal at the place where the comparison is made [Fig. 5(a)].
- 3) The phase of the reference signal is then locked.
- 4) The klystron is turned on, and the phase of the klystron wave in the accelerator section is compared with the reference signal.
- 5) The phase of the *klystron* signal is adjusted to be 180 degrees away from the phase of the reference signal [Fig. 5(b)].

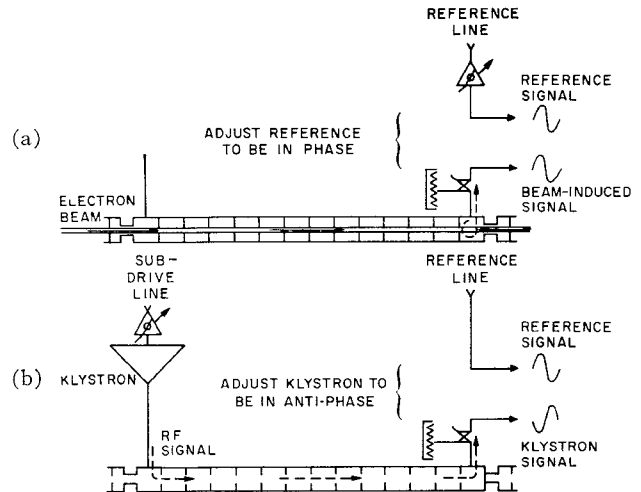


Fig. 5. Illustrating beam-induction method of phasing accelerator.

For the reasons explained before and illustrated in Figs. 3 and 4, the klystron is then optimally phased.

For clarity in the statement of the principle of operation, one oversimplification of the system was made which requires immediate correction: when the phase comparison between beam-induced and reference signals is being made, the klystron is not actually turned off but is simply delayed by about 50  $\mu$ s with respect to the beam. Thus, the average power dissipated in the accelerator section remains the same and thermal changes are avoided. The delayed position is hereafter called the “standby” position.

#### *Advantages and Problems of the Beam-Induction Technique*

The beam-induction method has a number of advantages but also poses certain problems that will be discussed later. The advantages are:

- 1) Of all the methods making use of the beam, it has the best sensitivity, particularly when the beam current becomes very small.
- 2) The beam and klystron signals are sampled directly at the accelerator, and are transmitted along a common cable to the phase detection circuit in the Klystron Gallery. The phase comparison is therefore essentially direct; the length of the cable does not need to be known, and the attainable sensitivity and accuracy are good.

- 3) There need be very little interference with physics experiments, because only one klystron at a time need be set to standby as the phasing operation progresses along the machine.
- 4) Klystrons which are placed on standby for reasons other than phasing can be maintained correctly phased with respect to the beam, so that they are instantly available for acceleration on demand.

Among the problems, the most serious relates to the very large difference between the power levels of the beam-induced and the klystron signals. We have to consider the extremes of the specified operating conditions under which the phasing system will be required to operate, viz., a beam current pulse as low as 1 mA, and a klystron peak power input to one 10-foot accelerator section as high as 24 MW. The attenuation per 10-foot section is approximately 5 dB, and the beam-induced power is 26 W/mA<sup>2</sup>, so that the largest power ratio of the two signals at the end of the 10-foot section is roughly 54 dB.

Well known devices such as the slotted line, "magic T" and hybrid ring are normally used as networks for the phase comparison of two signals. A minimum or a null in the detected output from one arm of these devices indicates a given phase relationship between the two signals. A null is obtained only if the two signals are of equal amplitude. As the difference between the amplitudes of the two signals increases, the phase-indicating null is replaced by a broad minimum, and the balance point becomes increasingly difficult to detect. The method is unreliable when the signals differ by more than 10 dB. Moreover, we require an *overall* phase detection system which will develop an error signal depending only upon the phase difference between the two input signals.

Let us consider then the performance of a hybrid ring used as a phase-comparison network (Fig. 6). The signals to be compared are applied to arms 1 and 2, arm 3 is terminated in a matched load, and a detector is placed

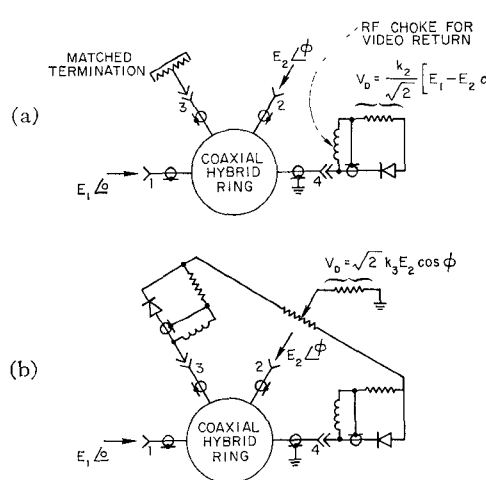


Fig. 6. Hybrid ring phase comparator.

on arm 4. Let the electric field amplitudes of the input signals be  $E_1$  and  $E_2$ . Then the output to the detector is given by

$$E_R^2 = \frac{E_1^2}{2} + \frac{E_2^2}{2} - E_1 E_2 \cos \phi \quad (5)$$

where  $\phi$  is the phase difference between  $E_1$  and  $E_2$  at arms 1 and 2.

Let  $E_2$  represent the reference signal and  $E_1$  either the beam-induced or the klystron signal.

If we use a square-law detector, the detector voltage  $V_D$  is

$$V_D = k_1 E_R^2 \quad (6)$$

so that

$$\begin{aligned} \delta V &= V_D |_{\phi+\pi} - V_D |_{\phi} \\ &= k_1 \left[ \left( \frac{E_1^2}{2} + \frac{E_2^2}{2} + E_1 E_2 \cos \phi \right) \right. \\ &\quad \left. - \left( \frac{E_1^2}{2} + \frac{E_2^2}{2} - E_1 E_2 \cos \phi \right) \right] \end{aligned} \quad (7)$$

or

$$\delta V = 2k_1 E_1 E_2 \cos \phi, \quad (8)$$

i.e.,

$$\delta V_{\max} = 2k_1 E_1 E_2. \quad (9)$$

Thus, with a square-law detector, the difference in voltage output for a given phase error is proportional to both  $E_1$  and  $E_2$ . We have seen that  $E_1^2$  can be expected to vary over a range of 54 dB, so that a square-law detector is very unsatisfactory.

Now, consider a linear detector, for which

$$V_D = k_2 E_R. \quad (10)$$

From (5),

$$E_{R(\max)} = \frac{E_1}{\sqrt{2}} \left[ 1 + \frac{E_2}{E_1} \right]. \quad (11)$$

It follows that

$$\begin{aligned} V_{D(\max)} - V_{D(\min)} &= \delta V_{(\max)} = k_2 \frac{E_1}{\sqrt{2}} \left[ \left( 1 + \frac{E_2}{E_1} \right) - \left( 1 - \frac{E_2}{E_1} \right) \right], \end{aligned}$$

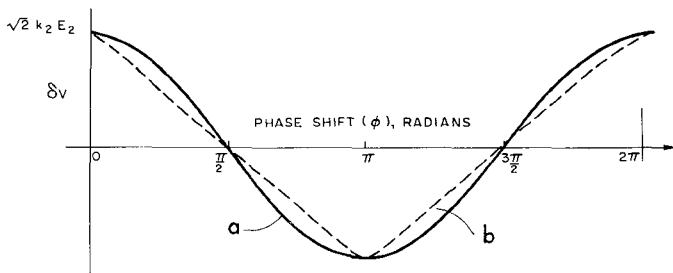
i.e.,

$$\delta V_{\max} = \sqrt{2} k_2 E_2. \quad (12)$$

This result is much more promising, since the voltage "swing," as the relative phase angle of the two signals is rotated, depends only on the amplitude of  $E_2$ , which can be kept constant.

In Fig. 7,  $\delta V$  is plotted as a function of the phase difference  $\phi$  in two cases. These are

- 1)  $E_1 \gg E_2$
- 2)  $E_1 = E_2$

Fig. 7.  $\delta V$  vs.  $\phi$  for linear diodes.

$$a = E_1 \gg E_2: \delta V = \sqrt{2} k_2 E_2 \cos \phi$$

$$b = E_1 = E_2: \delta V = \sqrt{2} k_2 E_2 (\cos \phi/2 - \sin \phi/2)$$

In Case 1), (5) becomes

$$E_R^2 \approx \frac{E_1^2}{2} \left[ 1 - \frac{2E_2}{E_1} \cos \phi \right] \quad (13)$$

so that

$$V_D \approx k_2 \frac{E_1}{\sqrt{2}} \left[ 1 - \frac{2E_2}{E_1} \cos \phi \right]^{1/2}$$

$$\approx \frac{k_2}{\sqrt{2}} [E_1 - E_2 \cos \phi]. \quad (14)$$

It follows that

$$V_D|_{\phi+\pi} - V_D|_{\phi} = \delta V = \sqrt{2} k_2 E_2 \cos \phi. \quad (15)$$

In case 2)

$$V_D = k_2 E_2 (1 - \cos \phi)^{1/2} \quad (16)$$

and

$$\delta V = 2k_2 E_2 \left( \cos \frac{\phi}{2} - \sin \frac{\phi}{2} \right). \quad (17)$$

Both cases give the same  $\delta V_{\max}$ .

The sensitivity,  $\partial(\delta V)/\partial\phi$ , is  $-\sqrt{2}k_2 E_2 \sin \phi$  in case 1), so that as  $\delta V \rightarrow 0$ , the sensitivity is  $-\sqrt{2}k_2 E_2$ .

In case 2)  $\partial(\delta V)/\partial\phi$  is

$$\sqrt{2} k_2 E_2 \left[ -\frac{1}{2} \sin \frac{\phi}{2} - \frac{1}{2} \cos \frac{\phi}{2} \right]$$

so that as  $\delta V \rightarrow 0$ , the sensitivity becomes  $-k_2 E_2$ . In other words, as we permit  $E_1$  to decrease from very large values to equality with  $E_2$ , the sensitivity of null detection decreases only by a factor  $1/\sqrt{2}$ .

We do not know of the existence of a detector which will remain perfectly linear over the specified range of input powers. The best approximation presently available is a coaxial thermionic diode, which maintains an index of less than 1.2 over the required range. It can be shown that when the detector has an index of 1.25 over a 50-dB power range, the detected output voltage will vary by 4 to 1 over that range. This variation is acceptable in our system.

The coaxial thermionic diode is mounted in a special

housing. The anode is held in position by spring fingers and connected to the center conductor of the Type  $N$  input RF connector. The detected output is taken from the cathode to a type TNC connector on the side of the diode housing. The filament power is supplied via a separate twinaxial connector.

Equation (14) shows that the diode output has a large component  $k_2 E_1/\sqrt{2}$  and a very small component  $k_2 E_2/\sqrt{2} \cos \phi$  which contains the phase error information. We can "cancel out" the unwanted large component by putting a second detector, identical to the first, on arm 3 of the hybrid ring and taking the difference between the two outputs.

The diode resistive loads are connected in opposition by a balancing potentiometer, the wiper of which may be adjusted to offset asymmetries in the hybrid ring, diodes and diode loads, reducing the  $E_1$  component to zero. At the same time the amplitude of the  $E_2 \cos \phi$  component is doubled.

In theory, the differential diode output, as described, contains the required phase information. If the diodes are balanced, then as the phase angle  $\phi$  rotates, the differential output will oscillate about zero, passing through zero when  $\phi = (n + \frac{1}{2})\pi$ . The direction from which zero is approached with increasing  $\phi$  may be used to avoid  $\pi$  ambiguity in phase setting. However, such a system, depending on dc balancing, is impracticable because of the long-term stability required of the diodes and the dc amplifiers. This problem is avoided by a "phase-wobbling" technique.

#### The Principle of "Phase-Wobbling"

The dc phase-detection system previously described is converted to an ac system by phase modulating the reference signal  $E_2$ . This artifice immediately removes most of the problems of drift in dc levels, and provides a method of instructing the automatic servo system whether the phase of  $E_1$  is leading or lagging the phase of the reference  $E_2$ .

Phase-wobbling is achieved by the use of a three-port switching circulator in the reference line (see Figs. 8 and 9). The reference signal enters through one port and propagates to the output port either directly or via a third port, depending upon the polarity of the field used to magnetize the ferrite material. The third port is terminated by an adjustable short-circuit, so that the difference between the two path lengths to the output port can be made one half-wavelength. The direction of current flow in the magnetizing coil is reversed before the arrival of each successive beam-induced or klystron RF pulse. Hence the CW reference signal  $E_2$  is "square-wave" phase modulated at 30 c/s so that successive beam-induced or klystron pulses are compared with reference signals which differ in phase by  $\pi$ .

The principle of the phase-wobbling technique is essential to the automatic phasing system which has been developed. Thus a description of the former introduces the main features of the latter.

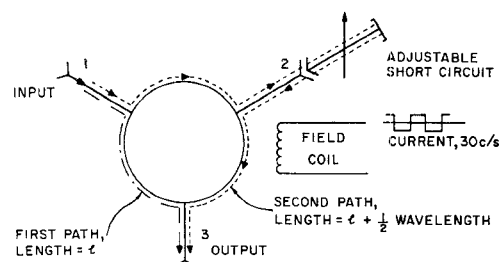


Fig. 8. Switching circulator used as phase wobbler.

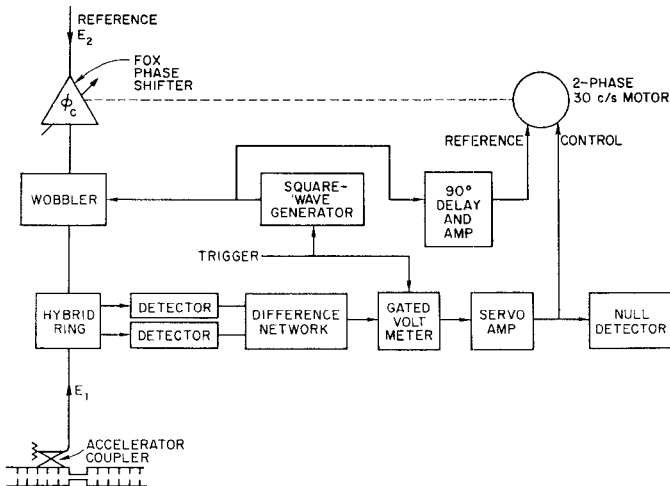


Fig. 9. Block diagram of phase-wobbling system.

A block diagram of the system is shown in Fig. 9. The CW reference signal  $E_2$  is transmitted to the wobbler via a Fox rotary phase-shifter. This type of phase-shifter was chosen because the phase shift it introduces is a linear, monotonically increasing function of the angle of rotation of the phase-shifter drum. There are no discontinuities or end-stops. The wobbler is driven by a 30 c/s square-wave generator, synchronized by a 60-pps trigger. The wobbler output is connected to the hybrid ring, where the accelerator signal  $E_1$  interacts with  $E_2$  as previously described. The output ports are terminated by the two thermionic diode detectors, and the differential output is fed into a gated voltmeter.

To understand the operation of the system so far described, we refer to both Fig. 9 and Fig. 10. Let the Fox phase-shifter be slowly rotated, so that the phase difference  $\phi$  between  $E_1$  and  $E_2$  at the hybrid ring increases from 0 to  $2\pi$  in a time  $2T_p$ , where  $2T_p$  is a few seconds [Fig. 10(a) and 10(b)]. The wobbler is phase-modulating  $E_2$  by  $\pm\pi/2$  at 30 c/s, so that the phase of  $E_2$  at the hybrid ring changes by  $\pi$  every 1/60 second. Pulses of signal  $E_1$  are arriving from the accelerator at the rate of 60 per second, the pulse length being 1 to 2.5  $\mu$ s. The trigger for the wobbler driver assures that  $E_2$  changes phase in the interval between the arrival of  $E_1$  pulses.

Equation (14) shows that the output from a single linear diode is  $k_2/\sqrt{2}[E_1 - E_2 \cos \phi]$ . Thus, the balanced differential output from two diodes will be  $\sqrt{2}k_2E_2 \cos \phi$ .

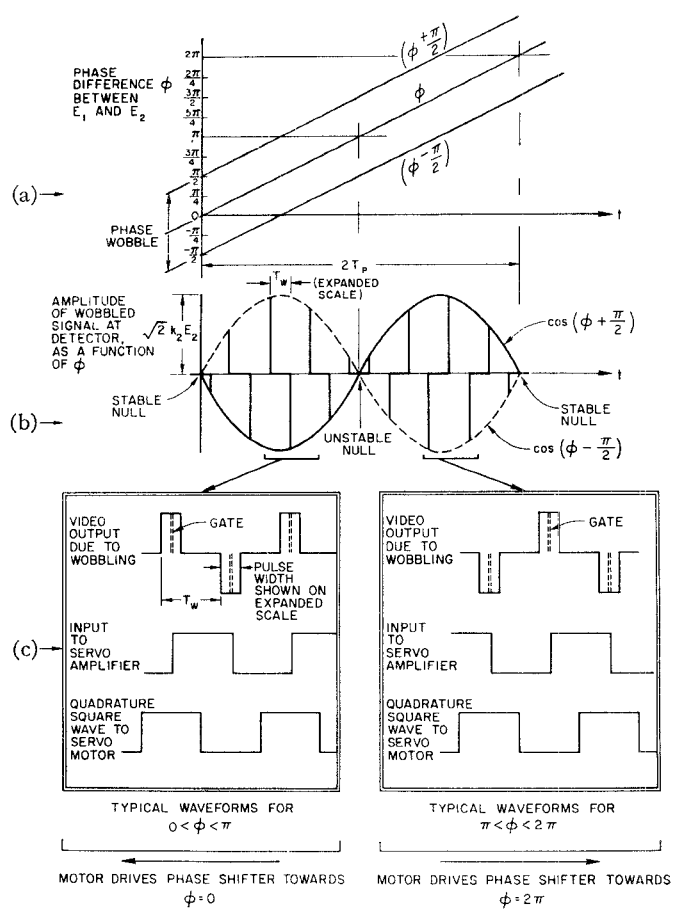


Fig. 10. Illustrating the application of phase wobbling to an automatic phasing system.

It follows that as  $E_2$  is wobbled, the differential diode output pulse amplitudes will change from

$$\sqrt{2}k_2E_2 \cos\left(\phi + \frac{\pi}{2}\right) \quad \text{to} \quad \sqrt{2}k_2E_2 \cos\left(\phi - \frac{\pi}{2}\right)$$

in a time  $T_W = 1/60$  second. (For clarity, the "wobbled" time scale in Fig. 10(b) has been expanded.)

To see what happens next, the output pulses are further expanded in the top line of Fig. 10(c). The pulse amplitudes are sampled by a "gate" 0.2  $\mu$ s wide. The sample is held until the next pulse arrives, so that a 30 c/s square wave is formed, with amplitude proportional to  $\cos[\phi + (\pi/2)]$ . This wave is amplified and fed to the control winding of a two-phase motor which drives the Fox phase-shifter.

Going back to the wobbler driver, part of the square-wave output is fed to a 90-degree delay circuit followed by an amplifier stage, giving a square-wave output which is in quadrature with the wobbler drive signal. This energizes the reference winding of the two-phase motor. Under these conditions, the motor will develop a torque proportional to the amplitudes of the applied square-waves. The direction of rotation will depend upon whether the control wave leads or lags the reference wave.

From Fig. 10(a) and (b), when  $0 < \phi < \pi$ ,

$$E_2 \cos \left( \phi + \frac{\pi}{2} \right) < 0 < E_2 \cos \left( \phi - \frac{\pi}{2} \right). \quad (18)$$

Therefore we connect the motor so that, under these conditions, the phase-shifter rotates towards  $\phi = 0$ .

It follows that when  $\pi < \phi < 2\pi$ ,

$$E_2 \cos \left( \phi + \frac{\pi}{2} \right) > 0 > E_2 \cos \left( \phi - \frac{\pi}{2} \right) \quad (19)$$

and the phase-shifter rotates towards  $\phi = 2\pi$ , which is identical with  $\phi = 0$ .

The system always drives away from the unstable null at  $\phi = \pi$  towards the stable null at  $\phi = 0$ .

Before proceeding to a description of the complete automatic phasing system, we shall digress briefly to point out further properties of the wobbler technique.

First, it can be shown that errors that would otherwise be introduced by differing diode characteristics are eliminated by phase-wobbling. This is an important advantage, because it is not possible to obtain a perfectly matched pair over the entire range of signal levels.

If the output voltages of the two diodes,  $A$  and  $B$ , on the hybrid ring are

$$V_A = k_A E_A$$

and

$$V_B = k_B E_B, \quad (20)$$

where  $E_A$  and  $E_B$  are the electric field amplitudes of the resultant RF waves in the output arms of the hybrid ring, then a simple analysis shows that the difference between the detected outputs in the two wobbler positions is zero when

$$\sqrt{2} E_2 (k_A + k_B) \cos \left( \phi + \frac{\pi}{2} \right) = 0. \quad (21)$$

This will be so when  $\phi = 0 \pm n\pi$ , independently of the values of  $k_A$  and  $k_B$ .

The second point to be made is that imperfections in the switching circulator do not affect phasing accuracy. It can be shown that if the phase difference introduced by switching from one path to the other is not exactly  $\pi$ , or if the two paths have different insertion losses, no phase error is introduced.

#### Overall Description of the Automatic Phasing System

Figure 11 is a schematic of the RF Drive System in one of the 30 sectors of the machine. The 476 Mc/s main drive signal is multiplied to 2856 Mc/s, at which point  $-10$  dB of the power is coupled off to provide the reference signal  $E_2$  for the phasing system. The remainder of the signal is used to drive the sub-booster amplifier, which feeds pairs of pulses (each  $2.5 \mu\text{s}$  long and separated by  $50 \mu\text{s}$ ) at 360 pulse-pairs per second

into the subdrive line. 60 pulse pairs per second are used for the phasing system.

The subdrive line runs the length of one sector. Power is coupled from it at eight points, each coupler feeding one main klystron through an isolator, phase-shifter, attenuator unit (Fig. 12). The phase-shifter in this unit is of the type already described. It is coupled to the automatic phasing system, and will be referred to as the "klystron phase-shifter,"  $\phi_k$ . The RF output from each klystron feeds four 10-foot accelerator sections, as shown. The lengths of waveguide runs between the klystron and the four sections are carefully controlled to give the correct phase relation between each section at the design frequency and temperature. No adjustment of the relative phases within each group of four sections is possible after installation. A 20-dB cross-guide coupler is used to sample the klystron wave and the beam-induced wave for phasing purposes.

Figure 13 is a block diagram of the automatic phasing system for an entire sector. The outputs from the third section of each group are transmitted to an eight-position switch which selects one channel at a time and transmits the  $E_1$  signal to the hybrid ring-wobbler-detector system which has been described previously. The switch, wobbler, and phase detector are housed in the "RF Detector Panel." The phase-shifter in the reference line to the wobbler is known as the "control phase shifter"  $\phi_c$ .

The gated voltmeter, servo amplifier, wobbler driver, 90-degree delay, and amplifier are housed in an "electronics panel" together with a "null detector" which determines when the phasing operation is complete by measuring the servo control voltage. The programmer is a special switching unit which ensures that the steps described in the previous section are carried out in sequence, and repeated "down the line" until all eight klystrons in one sector are properly phased.

The operation of the complete system is as follows:

- 1) When the programmer "start" button is pressed, klystron no. 1 is set to the standby pulse position (i.e., delayed  $50 \mu\text{s}$  with respect to the beam pulse). Switches in the RF detector panel connect the appropriate accelerator section output to the hybrid ring, and the phase of the beam-induced wave is compared with the reference signal.
- 2) The control phase-shifter  $\phi_c$  rotates toward a stable null until the servo amplifier output drops below 2.5 volts. The motor then stops and the null detector indicates that the programmer may advance to the "klystron-phase" position.
- 3) A brake is applied to  $\phi_c$ .
- 4) Provided that klystron no. 1 is operating properly, the gate of the gated voltmeter shifts to sample the standby klystron pulse, so that the phase of the klystron wave is compared with the reference.
- 5) The klystron phase-shifter  $\phi_k$  preceding klystron no. 1 is connected to the electronics panel by the

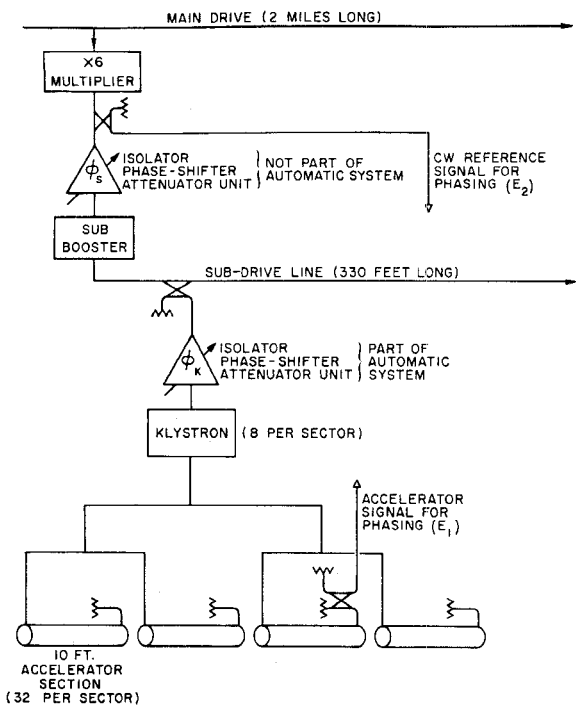


Fig. 11. Drive system schematic for one section of the machine, showing how the signals for the phasing system are derived.

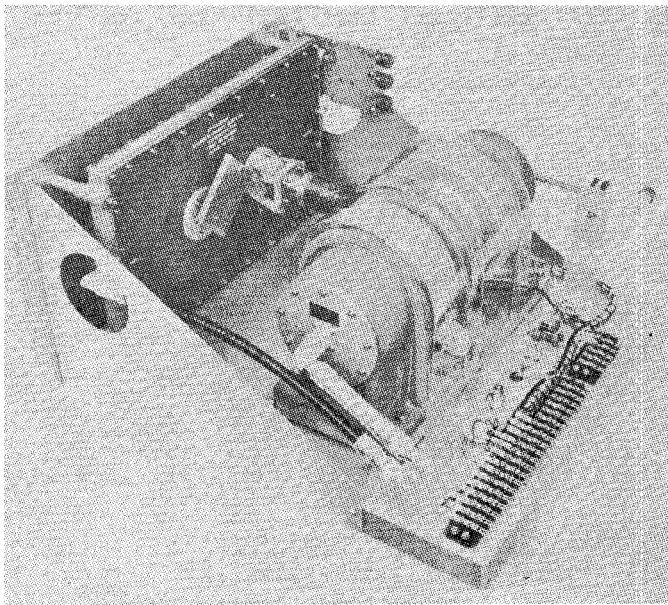


Fig. 12. An isolator, phase-shifter, attenuator unit.

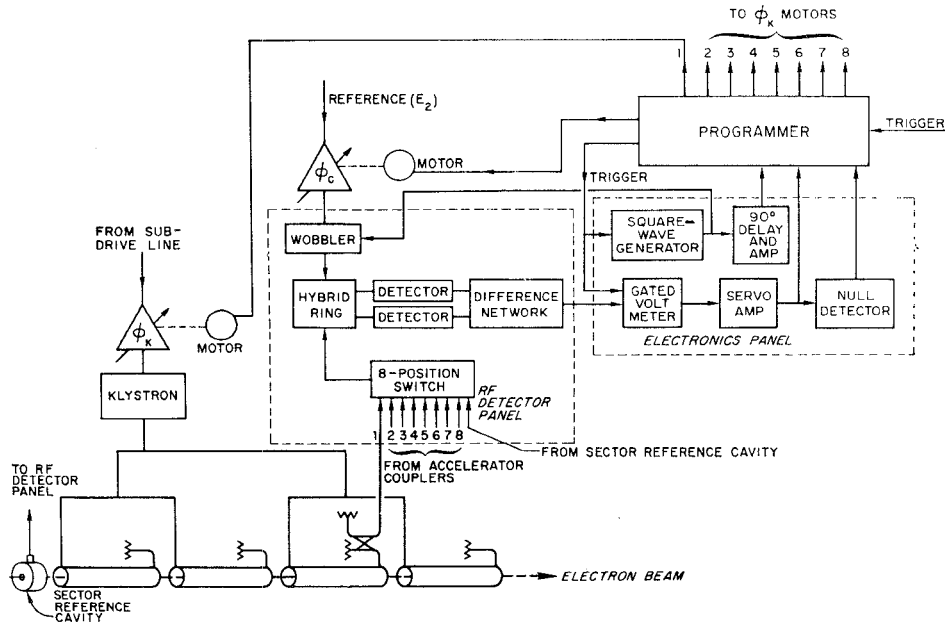


Fig. 13. Block diagram of automatic phasing system for one sector.

programmer and rotates to a stable null which is made to be  $\pi$  away from the stable null of  $\phi_c$  by simply reversing two of the leads to the  $\phi_k$  motor.

- 6) When the null detector indicates that the phasing error is within the accepted tolerance, the programmer switches to klystron no. 2, setting it to standby and returning no. 1 to accelerate. The phasing cycle is then repeated.
- 7) The phasing operation continues until all eight klystrons are phased.

#### Early Experimental Results

The automatic phasing system has been operating in the first two sectors of the machine since early February 1965. These two sectors, comprising 660 feet of the two-mile accelerator, are being used to evaluate the basic design of the accelerator and ancillary equipment, while the rest of the machine is being built. After some initial adjustments the automatic phasing system has worked very satisfactorily. The average time required to phase a sector which is initially random phased is about one

minute. A sector which has been previously phased can be "trimmed" in 43 seconds. Tests were also performed to determine the resetting accuracy of the system. All phase-shifters were marked after being automatically set. The entire sector was randomly phased manually and then automatically rephased. The worst error measured was 3 degrees, with most phase-shifters returning to within 1 degree of their previous positions.

In addition to performing the essential function for which it was designed, the phasing system is beginning to be recognized as a very useful diagnostic tool. For instance, if the beam-induced pulse is observed as phasing proceeds down a sector, sudden decreases in the pulse amplitudes between adjacent test points immediately indicate loss of beam due to local mis-steering. Subdrive line and klystron-phase jitter and a variety of other malfunctions in the drive system can be easily recognized.

#### ACKNOWLEDGMENT

The authors are indebted to Dr. R. B. Neal and D. J. Goerz for their initial contributions in formulating the

idea of beam-induction phasing, and to G. Jackson, Jr., J. R. Bordenave, P. V. Lee, and K. E. Holladay for their assistance in developing and testing the prototype system.

#### REFERENCES

- [1] R. Belbœch and C. B. Williams, "Current variation detection technique of phasing linear electron accelerators," Stanford Linear Accelerator Center, Stanford University, Internal Memorandum, November 1962.
- [2] W. J. Gallagher et al. (Drive and Phasing Committee), "Methods for phasing long linear accelerators," Stanford Linear Accelerator Center, Stanford University, Calif., Rept. M-101, November 1958.
- [3] W. J. Gallagher et al. (Drive and Phasing Committee), "Methods of driving long linear accelerators," Stanford Linear Accelerator Center, Stanford University, Calif., Rept. M-102, December 1958.
- [4] D. J. Goerz and R. B. Neal, "Phasing a linear accelerator from rf phase shift due to beam loading interaction," Stanford Linear Accelerator Center, Stanford University, Calif., Rept. M-103, December 1958.
- [5] R. B. Neal et al. (Drive and Phasing Committee), "Comparison of methods of phasing long linear accelerators," Stanford Linear Accelerator Center, Stanford University, Calif., Rept. M-104, December 1958.
- [6] R. B. Neal, "Transient beam loading in linear electron accelerators," Microwave Lab., Stanford University, Calif., Rept. ML-388, May 1957.
- [7] G. A. Loew, "Non-synchronous beam loading in linear electron accelerators," Microwave Lab., Stanford University, Calif., Rept. ML-740, August 1960.

# Stability and Gain Prediction of Microwave Tunnel-Diode Reflection Amplifiers

J. W. BANDLER

**Abstract**—The Nyquist approach to stability is used in a form suitable for representation on a chart having conventional Smith chart scales. It is shown how the gain and stability of negative conductance reflection amplifiers of the tunnel-diode type can be simultaneously predicted on this chart. The technique described is particularly useful in the practical design of these amplifiers embedded in networks having complicated functions of frequency, as it involves predominantly graphical computations. A procedure is outlined for constructing imittance curves for the tunnel-diode, viewed either as a series or as a parallel circuit. An example of a 3-Gc/s amplifier operating in a rectangular waveguide is given.

#### I. INTRODUCTION

A TUNNEL-DIODE, (Fig. 1), is potentially active at all frequencies from zero to resistive cutoff  $\omega_R$ , above which it is regarded as passive. For

Manuscript received March 11, 1965; revised May 4, 1965. The work reported in this paper was supported by the Science Research Council.

The author is with the Department of Electrical Engineering, Imperial College, London, England.

low-noise figures and wide-band performance, amplification is restricted to around or less than a third of  $\omega_R$ . Stability must, however, be considered over the whole active spectrum, and only when the effects of loading variations can be accounted for is it justifiable to concentrate on the desired amplification band.

Chapters VII-IX of Bode's book [1], especially the theorem on page 149, and the relevant parts of Henoch and Kvaerna's report [2] are useful in the following discussion. Also of interest are [3]–[6]. Poles  $P$  and zeros  $Z$  referred to in this paper are all contained in the r.h.  $p$ -plane. Real frequency loci are assumed to be plotted from just below  $-\omega_R$  to just above  $+\omega_R$ . The tunnel-diode equivalent circuit parameters are considered, for simplicity, to be frequency independent.

Figure 2 shows the Nyquist plots of two typical tunnel-diodes. Figure 2(a) converts to Fig. 2(b) on adding sufficient series resistance, and vice versa on adding